Study of Metal Additives to Alumina Substrate for High Temperature and Pressure Application

I Made Riko*[1], Stevin Snellius Pramana[1], Eric Phua Jian Rong[1,2], Wong Chee Cheong[1], Chen Zhong[1], Alfred Tok Iing Yoong[1], Gan Chee Lip**[1]
*imaderiko@e.ntu.edu.sg
** clgan@ntu.edu.sg

[1]School of Materials Science and Engineering, Nanyang Technological University, Singapore.
Block N4.1, 50 Nanyang Avenue, Singapore 639798

[2]Institute of Microelectronics, Singapore.
11 Science Park Road, Singapore Science Park II, Singapore 117685

Abstract

In this work, we present systematical characterizations of iron doped alumina substrates produced by solid state sintering of ball milled powders. It was found that the doped samples have higher fracture toughness, lower thermal conductivity, smaller coefficient of thermal expansion and higher relative dielectric constant than undoped ones. A reduction in thermal conductivity could arguably give extra protection to the package chip in a high temperature application environment and can be attributed to an increase in phonon scattering. Furthermore, the decrease in coefficient of thermal expansion also helps to reduce thermal induced stress between the substrates and device chip. The observed improvement in fracture toughness cannot be explained by the common toughening mechanism, such as crack bridging or due to the increase in crystallite size, and is the subject of further investigation.

Introduction

Electronic systems for extreme environments require highly reliable instrumentation and sensors that work in harsh conditions such as 2000 atm and temperature beyond 300°C. Such environment requires a different approach for microelectronics packaging. Operating at such extreme environment, selection of suitable device substrates is crucial, which needs to provide sufficient structural support for mounted devices and circuitries. It also requires to be electrically non-conductive to provide insulation for various conducting paths. Furthermore, substrates should be chemically stable and provide suitable thermal protection [1].

Ceramics based packages are commonly used as high temperature encapsulation. Unlike usual power devices, packaging materials for microelectronics devices operated under high temperature does not require to have a high thermal conductivity. For a power device that operates at relatively low ambient temperature (<125°C) [2], heat that is generated from the device chip has to be dissipated out to maintain optimum device's performance. On the other hand, high temperature microelectronics are typically low power devices that do not generate much heat to be dissipated to the environment. On the contrary, it is necessary to slow down the heat transfer from the environment to the device chip. Thus, for high temperature application device, it requires packaging solution that is not just mechanically strong, but also low in thermal conductivity to minimize heat transfer from the environment to the internal device. For this purpose, low thermal conductivity substrate could be more suitable.

In this study, Al_2O_3 is selected mainly due to its low thermal conductivity, good electrical insulating properties, chemically stable at high temperature and is a particularly mature technology and inexpensive to produce or acquire. However, it has a relatively high dielectric constant and high coefficient of thermal expansion (CTE) as compared to Si that may impose some reliability issues.

Substrate doping with other elements has been used to modify their mechanical and microstructure properties, for example tiny amount of MgO as a sintering additive [3–5]. On the other hand, introducing dopants could as well reduce the thermal conductivity of the substrates by mechanism of increasing phonon scattering centers.

Iron has been identified as a possible dopant for alumina substrates in such an application. For one, Fe doping has been reported to improve the alumina fracture toughness by means of crack bridging mechanism due to the presence of ductile iron phase [6–9]. Addition of Fe was also reported to decrease transformation temperature of amorphous alumina η phase to crystalline α alumina [7]. On top of that, the introduction of Fe is also reported to improve alumina - metal adhesion [10]. On the other hand, the addition of Iron can also be viewed as introducing more defects to the alumina matrix, thus increase the possibility of phonon scattering and therefore will reduce the thermal conductivity.

In this work, we present systematical characterizations of the iron doped alumina substrate produced by powder methods.

Experiment

A mixture of alumina with 10wt.% Iron (Fe) was prepared by wet ball milling (with 1:20 powder to ball ratio) in alumina ball milling jar for 24 hours. Comparisons between the particle size of as purchased alumina, iron-powder and post ball milling of alumina with 10wt.% Fe are given in Fig. 1(a) to (c), respectively. It can clearly be observed from secondary electron microscope (SEM) imaging that ball milling effectively reduces the particle size of the mixed powder. The resulting powder was uniaxially pressed to form pellets, followed by 200 MPa cold isostatic pressing. The resulting pellets were air sintered at 1500°C for 12 hours.

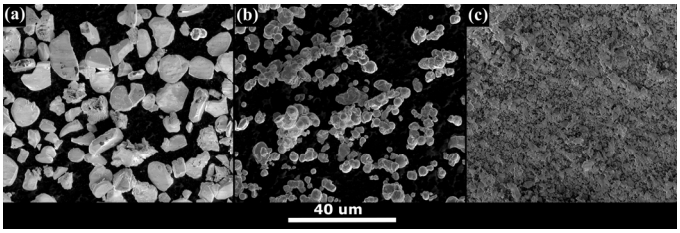

Fig. 1 Comparison of particle size. (a) As received alumina powder, (b) iron powder, and (c) ball milled mixture of alumina and iron powder.

Fracture toughness of the samples was deduced from the crack length measurement from Vickers indentation based on the following relation [11].

$$K_c = \xi_v^R \left(E/H\right)^{1/2} \left(P/c_o^{3/2}\right) \quad (1)$$

where P is the indentation peak load, c_o is the crack length, ξ_v^R = 0.016 ± 0.004 is a material-independent constant for Vickers produce radial cracks [11], E is the Young's modulus and H is the materials hardness defined as

$$H = P/a_o\, a^2 \quad (2)$$

where a is the half diagonal of indentation length and $a_o = 2$ is numerical constant for Vickers indenter.

Sintered samples were indented with Vicker's pyramid shaped tip micro-indenter with 10 kgf load setting for 10 s dwell time. Commercially purchased sintered alumina sample from Xellatech Pte. Ltd. were also measured and used as a reference.

Thermal conductivity of sintered sample was deduced from the thermal diffusivity measurement by laser flash method. Thermal diffusivity was indirectly measured by observing the temperature changes on the front side of the sample by laser illumination from the back of the sample. Thus, the thermal conductivity was obtained by the following relation [12]

$$k = \alpha\rho C \quad (3)$$

where α is the thermal diffusivity, ρ is the density and C is the specific heat of the specimen.

Thermal expansion coefficient was deduced from measured linear dimensions change with respect to increasing heating from 20°C to 400°C. Dielectric constant was obtained from impedance measurement of sintered samples at 1 MHz frequency using Agilent 4284 A LCR-Meter.

Bruker D8 Advance X-ray diffractometer (XRD) with CuK_α radiation was used for phase analysis of ball milled and sintered sample. Rietveld refinements were utilized for phase quantification from XRD diffraction patterns. Both the XRD characterisations and phase quantification were conducted at Facility for Analysis, Characterization, Testing and Simulation (FACTS) in Nanyang Technological University, Singapore.

Results and Discussion

Fig. 2 shows a comparison between indentation in the doped sample and reference sample. The diagonal of the indentation a and the crack length c_o, which are used as input parameters for fracture toughness calculation as shown in eq. (2), are indicated as a and c in Fig. 2(a) and (b), respectively. The doped sample clearly shows field of residual stress [13], but is not visible on the reference sample. Nonetheless, crack length on the reference sample is visible and measureable.

All measured properties are summarized in Table 1. It was found that doped samples have higher fracture toughness (6.12 ± 1.23 MPa/m$^{0.5}$) as compared to undoped reference samples (3.14 ± 0.88 MPa/m$^{0.5}$).

Both samples have similar mass density and are presented here as relative density with respect to their respective mixture theoretical density.

Doped samples also show a lower thermal diffusivity as compared to the reference sample, i.e. 5.11 ± 0.04 mm^2/s and 8.14 ± 0.09 mm^2/s, respectively. On the other hand, there seems to be no significant heat capacity difference between the two samples. From differential scanning calorimeter (DSC) heating and cooling curves, both samples have heat capacity of ~ 0.765 J/gK at 25°C. Thus from eq. (3), we calculated that there is a reduction in thermal conductivity of the doped sample from 22.43 ± 0.29 W/mK to 16.16 ± 1.91 W/mK).

Doped sample also shows a CTE reduction from 8.40 ± 0.017 ppm/K to 6.91 ± 0.048 ppm/K. On the other hand, the relative dielectric constant is higher for the doped sample (10.36 ± 0.241 as compared to 9.9 ± 0.018).

Reduction in thermal conductivity in doped sample is expected as introducing impurity means introducing defects to the alumina crystals. Crystal defects increase phonon scattering probability, thus reducing the thermal conductivity. However, it is unclear what mechanism causes the reduction in CTE and the fracture toughness change.

Compositional effect of Al_2O_3 and Fe_2O_3 can be ruled out as Fe_2O_3 has a higher CTE than the doped sample, i.e. 9.9 ppm/K [14]. Improvement in the doped sample fracture toughness can be traced to two possible mechanisms, the first of which is crack bridging mechanism by the presence of ductile Fe [8].

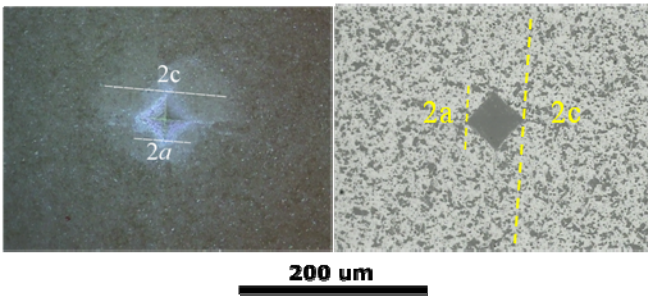

(a) **(b)**

Fig. 2 Vickers micro hardness indentation comparison between (a) doped sample and (b) reference sample.

Table 1 Summary of Measured Properties

Properties	Fe doped Alumina	Reference Alumina
Relative Density (%)	91.10 ± 0.57	90.90 ± 0.025
Fracture Toughness (MPa/$m^{0.5}$)	6.12 ± 1.23	3.14 ± 0.88
Thermal Conductivity (W/mK)	16.16 ± 1.91	22.43 ± 0.29
Relative Dielectric Constant	10.36 ± 0.241	9.9 ± 0.018
Coefficient Thermal Expansion (ppm/K)	6.91 ± 0.048	8.40 ± 0.017

For the crack bridging mechanism to work, it will require a high enough unoxidized Fe content available after sintering, which we have not detected in our investigations. The other mechanism is toughening by grain size increase promoted by Fe^{2+} [15].

During sintering, particularly air sintering, Fe will be oxidized and can be present either as Fe^{2+} or Fe^{3+}. Stößer *et al.* reported that Fe^{3+} had no effect on corundum formation [16], which implied that there was no effect to the sintering temperature and grain growth. On the other hand, the presence of Fe^{2+} has been associated with highly anisotropic grain growth of alpha-alumina [6], which implies that Fe^{2+} assists in diffusion. To verify which mechanism is operative, further characterizations by X-Ray diffraction (XRD) method were conducted.

XRD characterizations of as-prepared and sintered samples are given in Fig. 3(a) and (b), respectively. Rietveld refinement on the as-prepared powder shows that around 2.36 ± 0.14 wt % crystalline Fe remains in the form of Iron, Hematite (F_2O_3), Wüstite (FeO), from the 10 wt% Fe initially added. Reduction in the detected quantity of Fe can be attributed to both the formation of amorphous Fe, and addition of alumina. The source of extra alumina could come from erosion debris of the ball milling jar as well as the alumina ball during the ball milling process. Rietveld refinement also indicates that the average grain-size from Integrated Breath Volume weighted mean column lengths [17] (LVol-IB) is 50.20 ± 8.1 nm, as deduced from significant peak broadening.

The current powder preparation uses vertical ball mill, commonly known as Planetary Ball Mill, which could effectively mix and grind materials down to very small sizes.

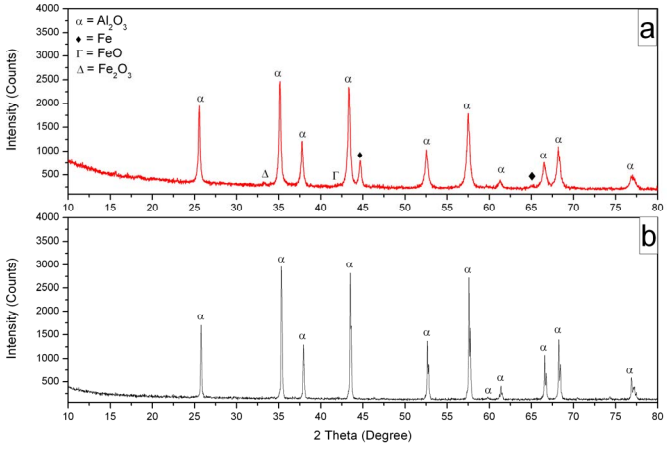

Fig. 3 X-Ray Diffraction characterizations of ball milled powder and after sintered powder. (a) Ball milled powder, consists of mixture of Al_2O_3, FeO, and Fe_2O_3. After ball milling, only 2.36 ± 0.14 wt% Fe is detected in the mixture, mostly caused by addition of alumina from milling jar and balls. (b) Sintered pallet, with 2.30 ± 0.04 at.% Fe in Fe^{3+} found to substitute Al^{3+}, which translates to ~2.5 wt.% Fe.

During milling, grinding balls in the jars are subjected to superimposed rotational movements, that differ in speeds between the balls (made of alumina) and grinding jars (also made of alumina), producing an interaction between frictional and impact forces. These high impact forces effectively reduce the particle size, and possibly amorphize the iron. At the same time, high impact of the balls to the milling jar also can erode both the jar and balls resulting in addition of alumina to the powder being milled. Hence, this reduces the iron weight percentage further.

On the other hand, the full width at half maximum observed from the XRD pattern of the sintered sample is narrower as compared to the powder state. Rietveld refinement on the sintered sample shows that all *hkl* reflections can be identified as Corundum Al_2O_3 phase with an average crystallite size (LVol-IB) of 122 ± 10 nm, an increase from 50.20 ± 8.1 nm for the unsintered powders. Neither Fe(bcc) nor other oxidized Fe was observed. The absence of Fe metal thus implies that the fracture toughness increase is not contributed by crack bridging mechanism. Further refinement shows that around ~2.5 wt% Fe (2.30 ± 0.04 at. % from Rietveld) has substituted for Al^{3+}. This substitution has made the unit cell slightly larger, with their lattice parameter changed from a = 4.7591 Å and c = 12.9973 Å to a = 4.7735 ± 8.8×10^{-4} Å and c = 13.0293 ± 3.8×10^{-4} Å, respectively. This result indicates that all available Fe have been oxidized to Fe^{3+} during sintering and none remains as Fe^{2+}. Furthermore this result indicates that none of the Fe was amorphized by ball milling.

It is common to observe increase in grain size as a result of heat treatment by mechanism of surface diffusion or bulk diffusion [18], which may lead to higher fracture toughness. Furthermore, increase in the grain size might also be enhanced by Fe^{2+} diffusion assisted grain growth. Even though there is no Fe^{2+} present after sintering, it may briefly be available during sintering before being oxidized to Fe^{3+}. In this relatively short time period, Fe^{2+} could induce the formation of oxygen vacancies to maintain charge balance in the crystal, which leads to faster diffusion path and induces faster grain growth, therefore larger grains after sintering [15]. On the other hand, effects of Fe^{2+} during sintering have been associated with formation of highly anisotropic grain growth, which is attributed to cause reduced density of the sintered body [19].

Conclusions

In summary, we have seen that Fe doped alumina could potentially be used as substrates for harsh environment electronic application. With comparable electrical properties, and potentially less CTE mismatch with silicon, usage of Fe doped alumina could lead to more reliable packaging solution. While the reduction in thermal conductivity can be attributed to an increase in phonon scattering, the observed improvement

in fracture toughness as well as reduction in CTE cannot be fully explained at the current stage, and are the subjects of further investigations.

Acknowledgments

The authors would also like to acknowledge SERC Grant No. 1021650081 for the support of this work. Authors also would like to acknowledge Dr S. Valavan from Republic Polytechnic Singapore for the access to thermal diffusivity measurement system.

References

[1] L. Coppola, D. Huff, F. Wang, R. Burgos, and D. Boroyevich, 'Survey on High-Temperature Packaging Materials for SiC-Based Power Electronics Modules', in *IEEE Power Electronics Specialists Conference, 2007. PESC 2007*, 2007, pp. 2234 –2240.

[2] 'Treatise Helps Users Interpret and Apply MIL-STD-810—A Test Method Standard', *Journal of the IEST*, vol. 48, no. 1, pp. 147–151, Sep. 2005.

[3] P. F. Becher, 'Microstructural Design of Toughened Ceramics', *Journal of the American Ceramic Society*, vol. 74, no. 2, pp. 255–269, Feb. 1991.

[4] S. I. Bae and S. Baik, 'Critical Concentration of MgO for the Prevention of Abnormal Grain Growth in Alumina', *Journal of the American Ceramic Society*, vol. 77, no. 10, pp. 2499–2504, Oct. 1994.

[5] T. Ikegami and Y. Moriyoshi, 'Evaluation of Grain-Growth Parameters', *Journal of the American Ceramic Society*, vol. 68, no. 11, pp. 597–603, Nov. 1985.

[6] P. Tartaj and J. Tartaj, 'Microstructural Evolution of Iron-Oxide-Doped Alumina Nanoparticles Synthesized from Microemulsions', *Chem. Mater.*, vol. 14, no. 2, pp. 536–541, 2002.

[7] X. Devaux, C. Laurent, and A. Rousset, 'Chemical synthesis of metal nanoparticles dispersed in alumina', *Nanostructured Materials*, vol. 2, no. 4, pp. 339–346, July.

[8] P. A. Trusty and J. A. Yeomans, 'The toughening of alumina with iron: Effects of iron distribution on fracture toughness', *Journal of the European Ceramic Society*, vol. 17, no. 4, pp. 495–504, Feb. 1997.

[9] J. Guichard, O. Tillement, and A. Mocellin, 'Preparation and characterization of alumina–iron cermets by hot-pressing of nanocomposite powders', *Journal of Materials Science*, vol. 32, no. 17, pp. 4513–4521, 1997.

[10] R. Kondou and T. Suga, 'Room temperature SiO_2 wafer bonding by adhesion layer method', in *Electronic Components and Technology Conference (ECTC), 2011 IEEE 61st*, 2011, pp. 2165 –2170.

[11] G. R. Anstis, P. Chantikul, B. R. Lawn, and D. B. Marshall, 'A Critical Evaluation of Indentation Techniques for Measuring Fracture Toughness: I, Direct Crack Measurements', *Journal of the American Ceramic Society*, vol. 64, no. 9, pp. 533–538, Sep. 1981.

[12] F. Boey, A. I. Y. Tok, Y. C. Lam, and S. Y. Chew, 'On the effects of secondary phase on thermal conductivity of AlN ceramic substrates using a microstructural modeling approach', *Materials Science and Engineering A*, vol. 335, no. 1–2, pp. 281–289, Sep. 2002.

[13] P. Chantikul, G. R. Anstis, B. R. Lawn, and D. B. Marshall, 'A Critical Evaluation of Indentation Techniques for Measuring Fracture Toughness: II, Strength Method', *Journal of the American Ceramic Society*, vol. 64, no. 9, pp. 539–543, Sep. 1981.

[14] S. B. Qadri, C. Fahed, H. Kim, A. Piqué, N. A. Mahadik, and M. V. Rao, 'Thermal expansion studies of indium–iron oxide', *Physica Status Solidi (B)*, vol. 248, no. 4, pp. 928–930, 2011.

[15] W. R. Rao and I. B. Cutler, 'Effect of Iron Oxide on the Sintering Kinetics of Al2O3', *Journal of the American Ceramic Society*, vol. 56, no. 11, pp. 588–593, Nov. 1973.

[16] R. Stößer, M. Nofz, M. Feist, and G. Scholz, 'Fe^{3+}-assisted formation of α-Al2O3, starting from sol–gel precursors', *Journal of Solid State Chemistry*, vol. 179, no. 3, pp. 652–664, Mar. 2006.

[17] H. M. Rietveld, 'A profile refinement method for nuclear and magnetic structures', *Journal of Applied Crystallography*, vol. 2, no. 2, pp. 65–71, Jun. 1969.

[18] R. L. Coble, 'Initial Sintering of Alumina and Hematite', *Journal of the American Ceramic Society*, vol. 41, no. 2, pp. 55–62, 1958.

[19] J. Zhao and M. P. Harmer, 'Sintering of Ultra-High-Purity Alumina Doped Simultaneously with MgO and FeO', *Journal of the American Ceramic Society*, vol. 70, no. 12, pp. 860–866, Dec. 1987.